第 48 卷 第 22 期/2021 年 11 月/中国激光 研究论文

中国激光

纳秒与飞秒激光作用下纳米金棒光热效应的理论与实验研究

赵鹏辉[1]，冯璟[1]，邢林庄[1]，李东[1*]，陈斌[1]，廖丁莹[2**]

[1]西安交通大学动力工程多相流国家重点实验室，陕西 西安 710049；

[2]西安交通大学第二附属医院眼科，陕西 西安 710004

摘要 纳米金颗粒可以有效增强激光诱导光学击穿效应，但不同脉冲激光下激光诱导光学击穿的机理不同。为了从微观角度揭示纳秒和飞秒激光照射纳米金颗粒过程中颗粒内部的光热转换和环境介质的变化，建立了脉冲激光加热水介质中纳米金棒的电子-声子双温度模型，结合实验研究，分析了不同激光能量密度和脉冲宽度对光热转换过程的影响，以及纳米金棒微观熔化特性的差异。结果显示，纳秒和飞秒激光照射下纳米金棒内部的电子和晶格温度的变化趋势基本一致。飞秒激光照射时纳米金棒的熔化阈值约为纳秒激光照射时的 1%，纳秒激光照射时纳米金棒周围的水温更高。飞秒激光照射时纳米金棒形貌的改变主要以机械碎裂为主，而纳秒激光作用下则主要以热致纳米金棒熔化为主。

关键词 激光技术；纳米金棒；激光诱导光学击穿；光热效应；电子-声子双温度模型

中图分类号 R318.51；R758.5 **文献标志码** A **doi**：10.3788/CJL202148.2202014

1 引 言

脉冲激光照射下的强电磁场可将材料电离击穿，这种现象称为激光诱导光学击穿(Laser induced optical breakdown，LIOB)。材料被击穿时产生等离子体，温度急剧上升，体积迅速膨胀，导致材料破坏。同时发射包含样品组分信息的光谱，通过分析等离子体光谱可以得到样品组分信息。目前，LIOB 已在生物样品检测、激光诱导击穿光谱及透明介质(玻璃等)的激光加工等领域中得到了广泛应用。直径在 1～100 nm 之间的纳米金颗粒[1](金纳米球[2-3]、金纳米棒[4]、金纳米笼[5]、金纳米壳[6]等)具有独特的局域表面等离子体共振(Localized Surface Plasmon Resonance，LSPR)特性[7]，可选择性地吸收特定波长激光的能量并转化为热能。基于这一特性，可利用纳米金颗粒介导增强 LIOB 效应。

近年来，关于纳米金颗粒[8]介导的激光诱导光学击穿的研究十分活跃。Arita 等[9]发现，脉冲激光照射下纳米金颗粒形成的 LIOB 效应可实现细胞光穿孔，使治疗性外源分子进入细胞，实现靶向治疗。Nedyalkov 等[10]发现，在纳米金颗粒介导下，可实现飞秒激光诱导硅基底表面纳米孔成型，实现精细化微纳加工。Boulais 等[11]针对飞秒脉冲激光辐照纳米金棒，建立了 LIOB 纳米金棒集总参数光热转化模型，揭示了超快脉冲激光辐照下纳米金棒附近水域等离子体生成与激光能量间的对应关系。Lachaine 等[12]基于激光辐照纳米金壳的集总参数光热转化模型，研究了纳米金粒子空间分布设计对纳米金粒子介导 LIOB 增强空化和细胞穿孔能力的影响。

纳米金颗粒介导的激光诱导光学击穿多采用纳秒或飞秒激光。在强脉冲能量照射下，纳米金颗粒的形貌可能会逐渐变成带有尖锐角和凸起边缘的不规则球形，导致其光热转换能力产生显著的变化[13]。然而现有研究多针对单一脉冲宽度开展，缺乏纳秒与飞秒激光作用下纳米金颗粒光热作用及形

收稿日期：2021-03-01；**修回日期**：2021-05-20；**录用日期**：2021-06-18

基金项目：国家自然科学基金(51976170)

通信作者：*lidong@mail.xjtu.edu.cn；**dingyingliao@163.com

貌变化的对比。从微观角度出发，深入揭示纳秒、飞秒激光照射纳米金颗粒过程中颗粒内部的光热转换规律，探究两种激光作用下纳米金颗粒形貌改变的机理，对于揭示纳米金颗粒介导的光学击穿机理具有重要指导意义。因此，本文构建了强脉冲激光照射纳米金棒的理论模型，研究了不同激光能量密度和脉冲宽度对光热转换过程的影响，结合激光照射纳米金棒的实验研究，分析了纳秒和飞秒激光下纳米金棒微观熔化特性的差异，为纳米金颗粒介导的 LIBO 应用提供了理论指导。

2　数理模型

2.1　控制方程

当纳米金颗粒受到强脉冲激光照射时，自由电子吸收的激光能量通过电子-晶格耦合传递至晶格，最后扩散到周围的介质中。由于激光脉宽较短（与金颗粒的热弛豫时间相当），需考虑纳米金电子与晶格间的非平衡传热，因此本文采用激光作用下的电子-声子双温度模型模拟纳米金棒在水中被强脉冲激光加热的过程[14]。纳米金棒自由电子和晶格在激光辐射影响下的瞬态传热过程为

$$C_{\mathrm{e}}\frac{\mathrm{d}T_{\mathrm{e}}}{d_{\mathrm{t}}}=g(T_{\mathrm{l}}-T_{\mathrm{e}})+\frac{E_{\mathrm{abs}}}{V\cdot\tau_{\mathrm{p}}},\tag{1}$$

$$C_{\mathrm{l}}\frac{\mathrm{d}T_{\mathrm{l}}}{d_{\mathrm{t}}}=g(T_{\mathrm{e}}-T_{\mathrm{l}})-\frac{Q_{\mathrm{w}}}{V},T_{\mathrm{l}}<T_{\mathrm{m}},\tag{2}$$

式中：T_{e} 和 T_{l} 分别为纳米金棒的电子温度和晶格温度；d_{t} 为时间间隔；C_{e} 和 C_{l} 分别为纳米金棒的电子和晶格的热容量；V 为纳米金棒的体积；τ_{p} 为激光脉冲宽度；Q_{w} 为纳米金棒与周围环境的热交换量；T_{m} 为纳米金棒的熔化温度；g 为计算传热的耦合因子；E_{abs} 为纳米金棒吸收的激光脉冲能量，取决于激光强度 F_{pulse} 和纳米金棒的吸收截面积 A_{abs}。(1)式右边第一项为电子和晶格的能量耦合，第二项为激光热源。(2)式右边第一项代表晶格和电子的能量耦合，第二项为纳米金棒和周围环境的热交换。其中 E_{abs} 的表达式为

$$E_{\mathrm{abs}}=A_{\mathrm{abs}}\cdot F_{\mathrm{pulse}}。\tag{3}$$

当纳米金颗粒被等离子体频率光线照射时，其有效吸收截面 A_{abs} 远大于几何吸收截面，可由离散偶极子近似理论（DDA）计算，过程详见文献[15]。

Q_{w} 为从纳米金棒到其周围环境的热损失率，可通过下式计算：

$$Q_{\mathrm{w}}=A_{\mathrm{s}}\cdot G\cdot(T_{\mathrm{l}}-T_{\mathrm{w}}),\tag{4}$$

式中：T_{w} 为纳米金棒表面的水温；G 为纳米金棒/流体界面的热导率；A_{s} 为纳米金棒的表面积。热导率 G 将界面处的温差与穿过界面的热通量相关联，$G=1.05\times10^{8}\ \mathrm{W\cdot m^{-2}\cdot K^{-1}}$[16]。

纳米金棒周围水的能量守恒方程采用圆柱坐标形式下的导热模型：

$$\rho_{\mathrm{w}}c_{\mathrm{p,w}}\frac{\partial T_{\mathrm{w}}}{\partial t}=\frac{\partial}{\partial Z}\left(k\frac{\partial T_{\mathrm{w}}}{\partial Z}\right)+\frac{1}{R}\frac{\partial}{\partial Z}\left(kR\frac{\partial T_{\mathrm{w}}}{\partial Z}\right),\tag{5}$$

式中：ρ_{w} 为水的密度；$c_{\mathrm{p,w}}$ 为水的比热容；R 为径向距离；Z 为纵向高度；k 为电子热导率；t 为激光作用时间。水和纳米金颗粒的能量方程通过热导率 G 实现耦合。

2.2　几何建模与网格划分

本文利用 Comsol 仿真软件，模拟了纳米金棒在水中被强脉冲激光加热的过程，研究了脉冲强度和脉宽等参数对纳米金棒内部光热转换和周围水传热过程的影响。参考典型双光子激光诱导击穿光谱成像[17]，本文计算采用的纳米金棒尺寸为 48 nm×14 nm。纳米金棒中心截面如图 1 所示，考虑对称性，本文将计算区域简化为二维轴对称结构，并设定二维圆柱坐标轴 R、Z。其中加粗实线以内区域为金纳米棒，加粗实线以外区域为包围着纳米金棒的水域。计算区域的网格划分如图 1(c)所示，纳米金棒与水传热密切的部分采用最小边长为 0.25 nm 的四边形网格，纳米金棒内部以及远离纳米金棒的水域则采用自由三角形网格，总网格数为 8219。

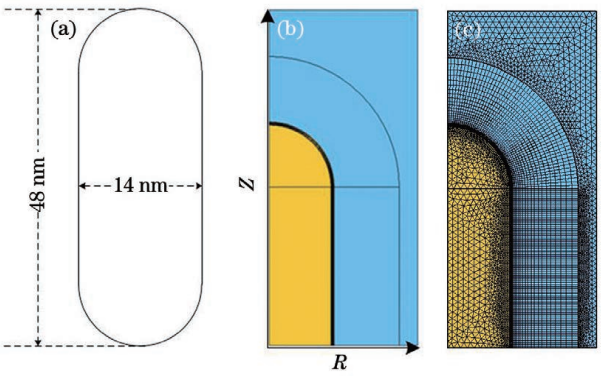

图 1　纳米金棒的形状与网格划分。(a)形状；(b)计算区域；(c)网格划分

Fig. 1　Shape of gold nano-rod and meshing. (a) Shape; (b) computing region; (c) meshing

2.3　初始条件和边界条件

双温度模型的控制方程(1)、(2)式分别用修正的欧拉方法进行数值求解。周围水的能量方程(5)式通过有限容积法进行空间离散，采用隐式格式进行时间离散，以获得时间和空间上的二阶精度。

模拟中取环境和纳米金棒的初始温度为 293 K，周围的水采用第二类边界条件。在进行数值计算以前，对计算区域的网格进行独立性考核，最终采用 0.032 nm 的网格和 1 fs、1 ns 的时间步长分别进行纳米金棒温度和水温的计算。水和纳米金的热物性如表 1 所示，其中 ρ_{gold} 为金的密度，k_{gold} 为金的导热系数，K 为水的导热系数，T_{cr} 为水的临界温度。

表 1　水和纳米金棒的热物性参数

Table 1　Thermophysical parameters of water and gold nano-rod

Parameter	Value
C_e /(J·m^{-3}·K^{-1})	$67.6T_e$
C_l /(J·m^{-3}·K^{-1})	$0.119+(3.061\times10^{-5})T_l$
g /(W·J·m^{-3}·K^{-1})	2.0×10^{16}
ρ_{gold} /(kg·m^{-3})	19300
k_{gold} /(W·m^{-1}·K^{-1})	320
T_m /K	1337
ρ_w /(kg·m^{-3})	1000
$c_{p,w}$ /(kJ·kg^{-1}·K^{-1})	4.184
K /(W·m^{-1}·K^{-1})	0.61
T_{cr} /K	647

3　模拟结果与讨论

3.1　模型的有效性验证

基于纳米金颗粒的电子-声子双温度模型，选定相应的初始值和物性参数，即可求解纳米金和周围水介质的温度场。文献[17]模拟了单个纳米金棒(48 nm×14 nm)在水介质中被 760 nm 飞秒激光辐照后纳米金棒电子和晶格温度以及周围的水温，其结果可用来验证本文模型的有效性。对比结果如图2所示，模拟采用的脉宽为 250 fs，脉冲能量为 4.7 J/m^2，均与文献[17]一致。

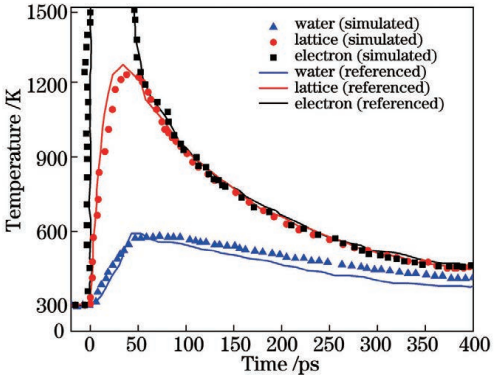

图 2　仿真结果与参考文献[17]结果的对比

Fig. 2　Comparison between simulated results and reference results

从图 2 中可以看出，本文模拟得到的纳米金棒电子和晶格温度以及周围水温的变化规律与文献[17]结果一致。电子温度在脉冲时间(250 fs)内持续上升，在脉冲结束时达到最大值。与随后的电子-声子和声子-声子耦合过程的皮秒时间尺度相比，这种快速的电子温度上升可以被视为瞬时过程。电子和晶格之间的热平衡发生在脉冲结束后 50 ps 左右。在脉冲结束后 500 ps 左右，纳米金棒表面和邻近水达到热平衡。上述对比结果说明本文提出的激光辐照熔化纳米金棒的模型是可靠的，可以用来预测激光照射下纳米金棒电子和晶格温度以及周围水温随时间的变化。同时计算结果也说明了计算飞秒尺度激光与纳米颗粒间的相互作用时采用电子-声子双温度模型的必要性。

3.2　激光脉冲宽度和强度的影响

利用(1)～(5)式可分别计算和对比不同脉宽激光与纳米金颗粒间的光热转化特性，并可研究激光参数包括脉冲强度、脉宽等对纳米金棒形貌的影响。根据本课题组前期研究结果[15]，48 nm×14 nm 的纳米金棒在 800 nm 激光照射下将获得最高光吸收。选取两种典型激光脉冲宽度即 100 fs 和 7 ns，纳米金棒和周围水的初始温度设置为 293 K。

首先研究飞秒激光照射下纳米金棒的光热转化特性，在脉宽为 100 fs、入射能量为 0.002 J/cm^2 的激光照射下纳米金棒电子和晶格与周围水的温度场分布如图 3 所示。从图 3 中可以看出，飞秒激光辐照后，纳米金棒内的自由电子率先吸收激光能量，进而导致电子温度升高。经过电子-晶格的驰豫，电子将热量传递给晶格。由于激光作用时间较短，晶格与电子未达到热平衡，因此电子温度远高于晶格温度。此外，由于激光作用时间短暂，晶格还未将能量传递至周围环境，因此周围水温显著低于纳米金棒温度。

图 4 为相同条件下纳米金棒晶格温度沿 Z 轴和 R 轴的分布随飞秒激光入射能量的变化，其中横虚线代表纳米金棒的熔化温度。可以看出：纳米金棒中心的温度较高，且随着激光功率密度的增加而上升。纳米金棒两端温度稍低，与中心的温度相差 60 K。纳米金棒外的水温温升较小，约为 10 K。模拟结果表明，激光带来的大部分能量被纳米金棒选择性吸收，升温后的纳米金棒对周围水的热量传递比较小。

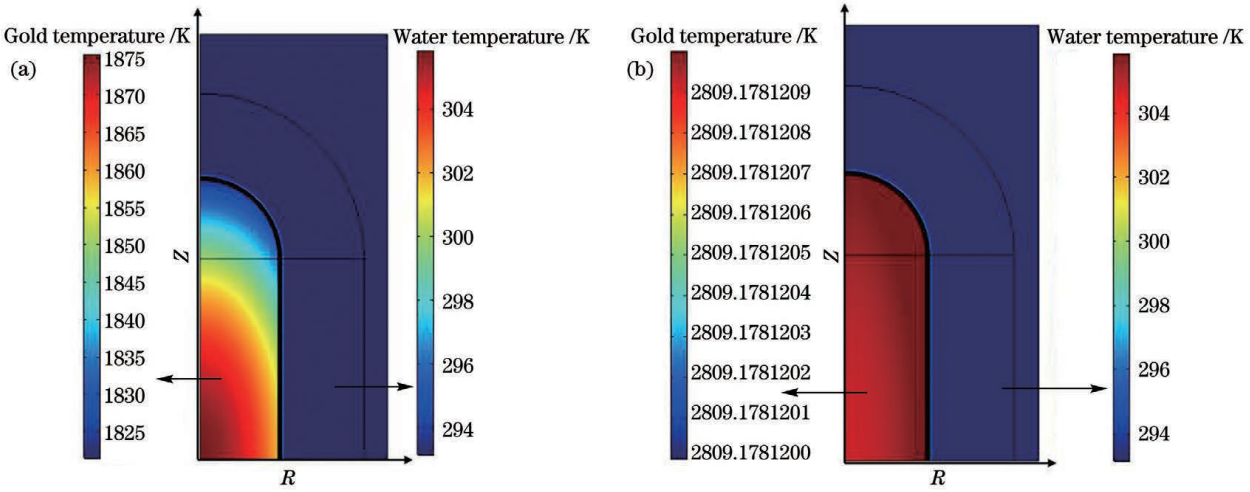

图 3 激光能量密度为 0.002 J/cm^2 时纳米金棒的温度分布。(a)晶格温度;(b)电子温度

Fig. 3 Temperature distributions of gold nano-rod at laser energy density of 0.002 J/cm^2. (a) Lattice temperature; (b) electron temperature

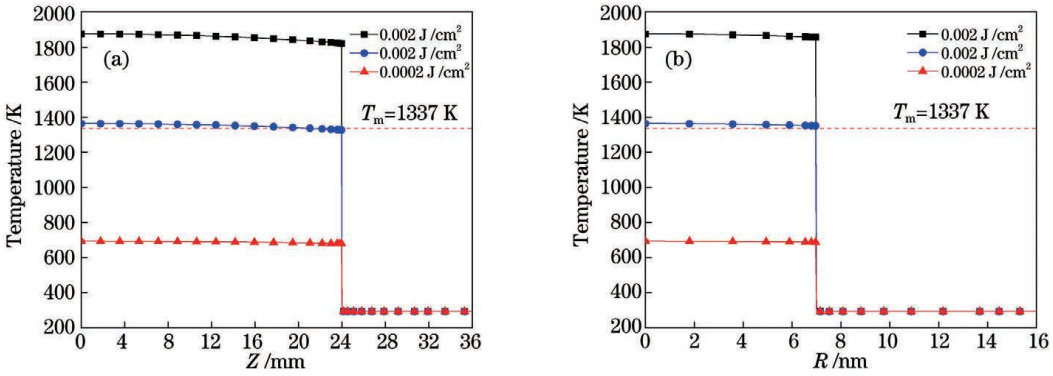

图 4 不同飞秒激光入射能量下的纳米金棒晶格温度分布。(a)沿 Z 轴;(b)沿 R 轴

Fig. 4 Lattice temperature distributions of gold nano-rod under different incident femtosecond laser energies. (a) Along Z axis; (b) along R axis

为了与飞秒激光进行对比,本文模拟了纳秒激光照射下纳米金棒的光热转化特性。在脉宽为 7 ns、入射能量为 0.8 J/cm^2 的激光照射下,纳米金棒电子和晶格与周围水的二维温度场分布如图 5 所

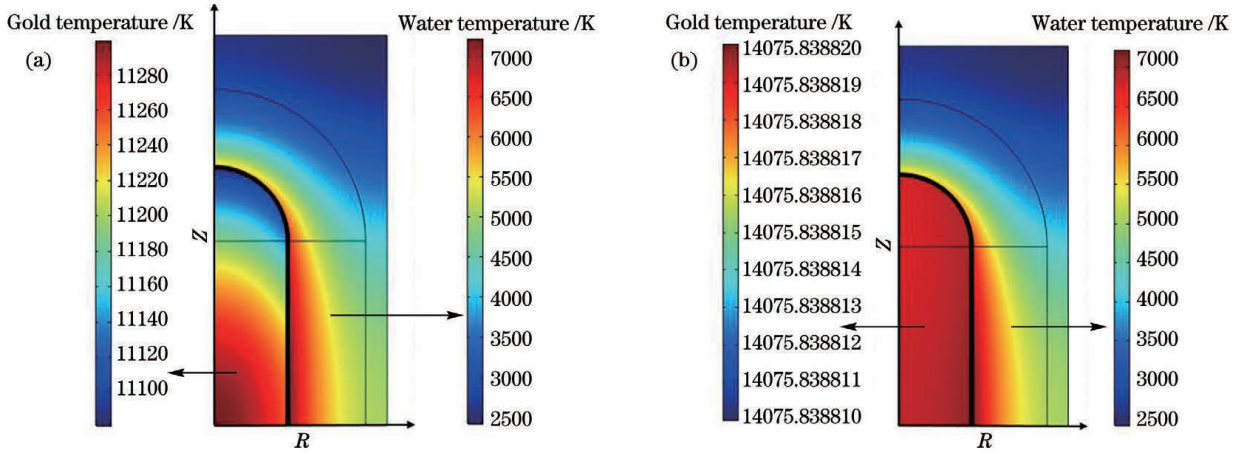

图 5 激光能量密度为 0.8 J/cm^2 时 纳米金棒的温度分布。(a)晶格温度;(b) 电子温度

Fig. 5 Temperature distributions of gold nano-rod at laser energy density of 0.8 J/cm^2. (a) Lattice temperature; (b) electron temperature

示。可以看出，在纳秒激光照射下，脉冲宽度显著延长，纳米金棒内晶格与自由电子的温差相比于飞秒激光照射情况显著降低，而周围水温显著增高。

纳米金棒晶格温度沿 Z 轴和 R 轴的分布随纳秒激光入射能量的变化如图 6 所示，其中横虚线代表纳米金棒的熔化温度。可以看出：在纳秒激光照射下，纳米金棒内部的电子和晶格温度的变化趋势和飞秒激光照射下的情况基本一致。纳米金棒内部的温度较为均匀，纳米金棒中心晶格的温度随着激光能量密度的增大而升高。棒内晶格温度从内到外递减，纳米金棒中心温度最高，棒端温度最低，纳米金棒中心和棒端的温度之差大约为 180 K。纳秒激光作用下纳米金棒周围的水温由于晶格的热量传递显著升高，但由于纳秒激光作用时间有限，因此纳米金棒外部水温受热影响的区域较小。从图 6 中可以看出，纳米金棒受热熔化的能量阈值约提高至 0.1 J/cm^2。对比飞秒激光和纳秒激光照射下纳米金棒的光热转化特性，可以发现，飞秒激光照射纳米金棒熔化的阈值（约为 0.001 J/cm^2）比纳秒激光照射时（约为 0.1 J/cm^2）降低了 99%，与实验结果[17]相吻合。

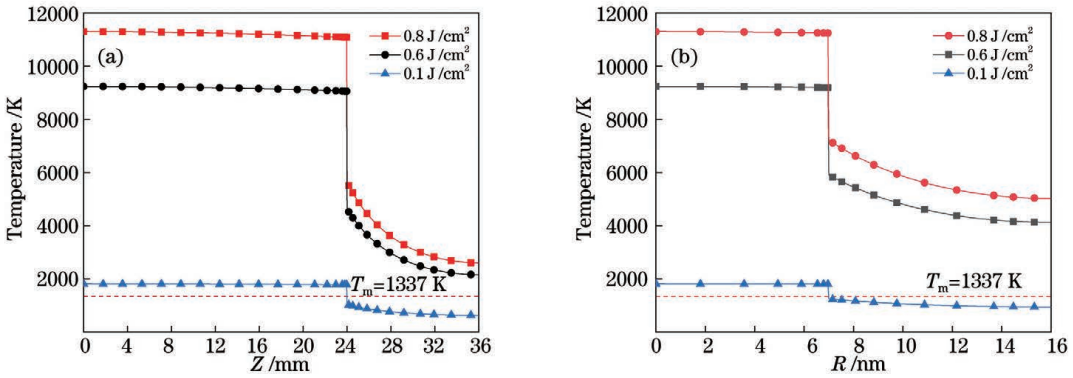

图 6　不同纳秒激光入射能量下的纳米金棒晶格温度分布。(a)沿 Z 轴；(b)沿 R 轴

Fig. 6　Lattice temperature distributions of gold nano-rod under different incident nanosecond laser energies. (a) Along Z axis; (b) along R axis

4　模拟结果与文献实验结果的对比分析

将本文模拟结果与文献[14]中的实验结果进行对比，进一步说明不同脉宽激光照射下纳米金颗粒光热转化特性的差异。文献[14]使用波长为 800 nm，脉冲宽度分别为 7 ns 和 100 fs 的激光照射纳米金棒。纳米金棒采用电化学法制备，照射前后的光谱特性和形貌分别由紫外-可见-红外光谱仪和透射电子显微镜（TEM）表征，制备的纳米金棒尺寸为 44 nm×11 nm。上述实验所使用的激光参数与本文模拟参数相同，纳米金棒尺寸与本文接近。

图 7 为文献[14]中不同入射能量密度纳秒激光照射后纳米金棒的 TEM 图。图 8 为文献[14]中不同入射能量密度飞秒激光照射后纳米金棒的 TEM 图。从图 7 中可以看出，激光辐照引起了纳米金棒表面的熔化。随着激光能量密度的增加，纳米金棒熔化成纳米金球的数量增多。能量增大到一定程度后，纳米金棒将完全等体积熔化为纳米金球。当激光能量密度继续增大时，纳米金球将熔化为粒径更

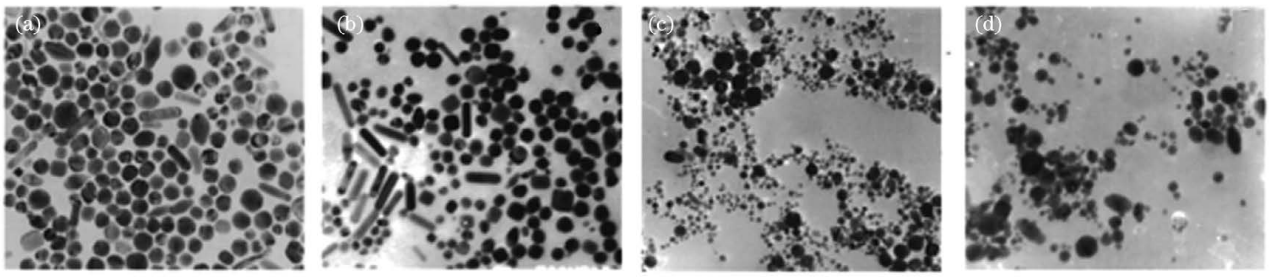

图 7　不同激光能量密度纳秒激光照射后纳米金棒的 TEM 图[14]。(a) 0.64 J/cm^2；(b) 0.8 J/cm^2；(c) 4 J/cm^2；(d) 16.7 J/cm^2

Fig. 7　TEM images of gold nano-rod irradiated by nanosecond laser with different laser energy densities [14]. (a) 0.64 J/cm^2; (b) 0.8 J/cm^2; (c) 4 J/cm^2; (d) 16.7 J/cm^2

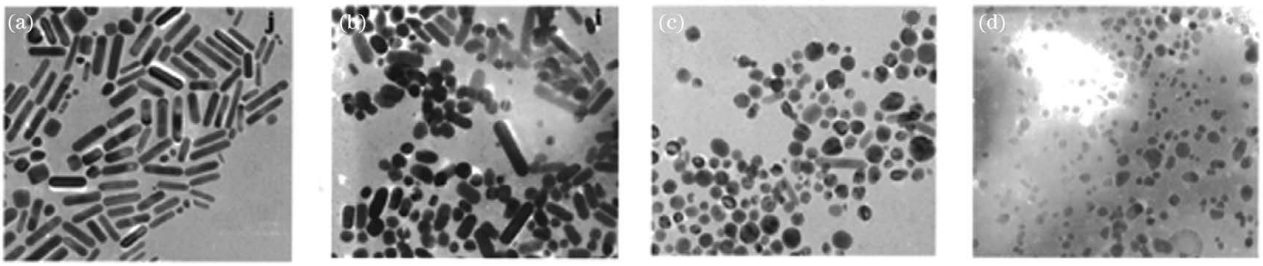

图 8 不同激光能量密度飞秒激光照射后纳米金棒的 TEM 图[14]。(a) 0.0002 J/cm^2;(b) 0.001 J/cm^2;(c) 0.56 J/cm^2;(d) 10.2 J/cm^2

Fig. 8 TEM images of gold nano-rod irradiated by femtosecond laser with different laser energy densities [14]. (a) 0.0002 J/cm^2; (b) 0.001 J/cm^2; (c) 0.56 J/cm^2; (d) 10.2 J/cm^2

小的球体。从图 8 中可以看出,较低的激光能量密度辐照已经引起了纳米金棒形貌的改变。当激光能量密度增加至与照射纳米金棒的纳秒激光能量密度接近时,纳米金棒破碎后形成带有尖锐角和凸起边缘的不规则球形,这一形貌特征与纳秒激光照射下的情况(图 7)显著不同。而当能量密度继续增大时,不规则纳米金球继续破碎为更小的粉末状。

上述实验结果可以根据本文模拟结果进行初步阐述。从图 3~6 可以看出,当 0.001 J/cm^2 飞秒激光照射激光纳米金棒时,达到熔化阈值时纳米金棒将发生熔化,但此时纳米金棒周围水温远低于金棒熔化温度,纳米金棒与水界面处的温差高达 1100 K,如此大的温差导致纳米金棒表面和内部不能在同一时刻发生热膨胀体积变化。各部分体积变化差异导致的相互牵制形成巨大的内应力,进而导致纳米金棒容易从内部开始产生点缺陷和线缺陷,然后演变成平面缺陷,最终发生断裂。而当 0.1 J/cm^2 纳秒激光作用于纳米金棒,温度达到熔化阈值时,纳米金棒周围水温与金棒熔化温度相当,纳米金棒与水界面的温差为 550 K,远低于飞秒激光加热情况,此时纳米金棒表面的热应力显著降低,不易发生破碎,因此主要通过热熔化形成纳米金球。

在实验中选用飞秒和纳米激光照射纳米金棒时,选用的激光能量密度略高于模拟结果。一方面,模拟中并未考虑激光透过水溶液所发生的能量耗散;另一方面,实验中激光作用于纳米颗粒群,激光能量密度需求显然高于单颗粒。

5 结 论

从微观角度分析了激光照射纳米金颗粒过程中颗粒内部的光热转换和对环境介质的影响,阐明了不同激光参数下纳米金棒微观熔化特性的差异。结果表明:在纳秒激光照射下,纳米金棒内部的电子和晶格温度的变化趋势与飞秒激光照射下的情况基本一致。但由于纳秒激光照射下脉冲宽度显著延长,因此相比于飞秒激光照射,纳米金棒内晶格与自由电子的温差显著降低,而周围水温显著增高。由于在更高的峰值功率下晶面容易产生缺陷,飞秒激光照射纳米金棒熔化的阈值(约为 0.001 J/cm^2)比纳秒激光照射时(约为 0.1 J/cm^2)降低了 99%。通过对比飞秒和纳秒激光照射纳米金棒的实验,进一步分析了不同脉冲激光照射下纳米金颗粒光热转化特性的差异。结果表明,当纳米金棒温度达到阈值时,飞秒激光照射纳米金棒是通过碎裂的形式发生形状改变,而纳秒激光照射纳米金棒则是通过热熔化的形式发生形貌变化。研究结果对强脉冲激光烧蚀金属材料实验有很重要的指导意义。

参 考 文 献

[1] Xing L Z, Li D, Chen B, et al. Preparation of nano gold colloid and its effect on blood light absorptivity [J]. Chinese Journal of Lasers, 2015, 42(6): 0604002.
邢林庄, 李东, 陈斌, 等. 纳米金胶体的制备及其对血液光吸收性的影响[J]. 中国激光, 2015, 42(6): 0604002.

[2] Lv H, Xu D, Henzie J, et al. Mesoporous gold nanospheres via thiolate-Au(i) intermediates [J]. Chemical Science, 2019, 10(26): 6423-6430.

[3] Yao C P, Zhang Z X. Influence of laser parameters on permeability of gold nanaoparticles targeting cells [J]. Acta Optica Sinica, 2009, 29(6): 1609-1615.
姚翠萍, 张镇西. 激光参数对纳米金靶向细胞膜通透性的影响[J]. 光学学报, 2009, 29(6): 1609-1615.

[4] Ruff J, Steitz J, Buchkremer A, et al. Multivalency of PEG-thiol ligands affects the stability of NIR-absorbing hollow gold nanospheres and gold nanorods

[J]. Journal of Materials Chemistry B, 2016, 4(16): 2828-2841.

[5] Sun H P, Su J H, Meng Q S, et al. Cancer cell membrane-coated gold nanocages with hyperthermia-triggered drug release and homotypic target inhibit growth and metastasis of breast cancer[J]. Advanced Functional Materials, 2020, 30(15): 1910230.

[6] Shabaninezhad M, Ramakrishna G. Theoretical investigation of size, shape, and aspect ratio effect on the LSPR sensitivity of hollow-gold nanoshells[J]. The Journal of Chemical Physics, 2019, 150(14): 144116.

[7] Ghosh S K, Pal T. Interparticle coupling effect on the surface plasmon resonance of gold nanoparticles: from theory to applications[J]. Chemical Reviews, 2007, 107(11): 4797-4862.

[8] Yang Y, Weng G J, Zhao J, et al. Progresses of preparation and applications of paper-based surface-enhanced Raman scattering substrate[J]. Chinese Journal of Lasers, 2018, 45(3): 0307011.
杨玥, 翁国军, 赵婧, 等. 纸质表面增强拉曼散射基底的制备及其应用进展[J]. 中国激光, 2018, 45(3): 0307011.

[9] Arita Y, Ploschner M, Antkowiak M, et al. Laser-induced breakdown of an optically trapped gold nanoparticle for single cell transfection[J]. Optics Letters, 2013, 38(17): 3402-3405.

[10] Nedyalkov N N, Miyanishi T, Obara M. Enhanced near field mediated nanohole fabrication on silicon substrate by femtosecond laser pulse[J]. Applied Surface Science, 2007, 253(15): 6558-6562.

[11] Boulais É, Lachaine R, Meunier M. Plasma-mediated nanocavitation and photothermal effects in ultrafast laser irradiation of gold nanorods in water[J]. The Journal of Physical Chemistry C, 2013, 117(18): 9386-9396.

[12] Lachaine R, Boutopoulos C, Lajoie P Y, et al. Rational design of plasmonic nanoparticles for enhanced cavitation and cell perforation[J]. Nano Letters, 2016, 16(5): 3187-3194.

[13] Ercolessi F, Andreoni W, Tosatti E. Melting of small gold particles: mechanism and size effects[J]. Physical Review Letters, 1991, 66(7):911-914.

[14] Link S, Burda C, Nikoobakht B, et al. Laser-induced shape changes of colloidal gold nanorods using femtosecond and nanosecond laser pulses[J]. The Journal of Physical Chemistry B, 2000, 104(26): 6152-6163.

[15] Xing L, Li D, Chen B, et al. Enhancement of light absorption by blood to Nd: YAG laser using PEG-modified gold nanorods[J]. Lasers in Surgeryand Medicine, 2016, 48(8): 790-803.

[16] Plech A, Kotaidis V, Grésillon S, et al. Laser-induced heating and melting of gold nanoparticles studied by time-resolved X-ray scattering[J]. Physical Review B, 2004, 70(19): 195423.

[17] Ekici O, Harrison R K, Durr N J, et al. Thermal analysis of gold nanorods heated with femtosecond laser pulses[J]. Journal of Physics D: Applied Physics, 2008, 41(18): 185501.

Theoretical and Experimental Investigations on Photothermal Effect of Gold Nanorods Irradiated by Femtosecond or Nanosecond Laser

Zhao Penghui[1], Feng Jing[1], Xing Linzhuang[1], Li Dong [1*], Chen Bin[1], Liao Dingying [2**]

[1] *State Key Laboratory of Multiphase Flow in Power Engineering, Xi'an Jiaotong University, Xi'an, Shaanxi* 710049, *China*;

[2] *Department of Ophthalmology, The Second Affiliated Hospital, Xi'an Jiaotong University, Xi'an, Shaanxi* 710004, *China*

Abstract

Objective At present, laser-induced optical breakdown has been widely used in biological sample detection, manipulation, laser-induced breakdown spectra and laser processing of transparent media (glass, etc.). Using the local plasma resonance effect of gold nanoparticles, the laser-induced optical breakdown effect can be enhanced by gold nanoparticles. Under the laser irradiation with strong pulse energy, the morphology of gold nanoparticles may gradually change into irregular spheres with sharp angles and convex edges, leading to significant changes in their photothermal conversion abilities. From the microscopic point of view, it is of great guiding significance to reveal the photothermal conversion rule inside gold nanoparticles in the process of nanosecond or femtosecond laser irradiation

and to explore the mechanism of the morphology change of gold nanoparticles under the action of two kinds of lasers. In this paper, a theoretical model of high intensity pulsed laser irradiation of gold nanorods is constructed to study the effects of laser energy density and pulse duration on the photothermal conversion process. Combined with the experimental study of laser irradiation of gold nanorods, the difference in the microscopic melting characteristics of gold nanorods under nanosecond or femtosecond laser irradiation is analyzed.

Methods In this paper, the electron-phonon dual temperature model under the action of laser is used to simulate the heating process of gold nanorods in water by intense laser pulses. Firstly, the basic properties of each domain are strictly defined, including the initial temperatures of gold nanorods and surrounding environment and the selection of boundary conditions for the surrounding water. The electron and lattice temperature variations are obtained by solving the governing equations based on the two-temperature model. According to the solved values of electron and lattice temperatures, we can use the energy conservation equation of water to obtain the transient changes of water temperature along the R and Z axes. By changing the pulse duration time and energy density of the laser, we can calculate the changes in lattice temperature and water temperature of the gold nanorods to compare with the experimental results.

Results and Discussions After the femtosecond laser irradiation, the free electrons in the gold nano-rods first absorb the laser energy, leading to the temperature rise of electrons. After electron-lattice relaxation, the electrons transfer heat to the lattice. Because the laser action time is short, the lattice and electrons do not reach a thermal balance, so the electron temperature is much higher than the lattice temperature. In addition, the energy has not been transferred to the surrounding environment, so the surrounding water temperature is significantly lower than that of the gold nano-rods. The pulse duration is significantly prolonged under the nanosecond laser irradiation, the temperature difference between the lattices and the free electrons in gold nanorods is significantly reduced compared with that under femtosecond laser irradiation, and the surrounding water temperature is significantly increased.

Comparing gold nanorods irradiated by nanosecond laser and those irradiated by femtosecond laser, we can find that when the gold nanorods are irradiated by 0.001 J/cm^2 femtosecond laser, the gold nanorods will be melt, but at the moment, the temperature of gold nanorods around the water is far lower than the melt temperature of the gold nanorods, and the temperature difference between gold nanorods and water is as high as 1100 K. Such a large temperature difference results in that the surface and interior of the gold nanorods cannot change in thermal expansion volume at the same time. The huge internal stress is formed due to the different volume change of each part. As a result, the gold nanorod is prone to produce point defects and line defects from the inside, and these defects subsequently evolve into plane defects and then nanorods fracture. When the 0.1 J/cm^2 nanosecond laser is applied to the gold nanorod and makes it melt above threshold, the gold nanorod melt temperature, the water temperature around the interface of gold nanorods and the water temperature are 550 K, far below the femtosecond laser heating threshold. The gold nanorod surface thermal stress is significantly reduced and the gold nanorods are not easily broken.

Conclusions In this paper, the theoretical and experimental studies are carried out to analyze the photothermal conversion inside gold nanoparticles and the influence on environmental media during laser irradiation from the microscopic point of view. The results show that the changes in electron and lattice temperatures under nanosecond laser irradiation are basically the same as those under femtosecond laser irradiation. However, compared with those under femtosecond laser irradiation, the temperature difference between the lattices and the free electrons in the gold nanorods is significantly reduced and the surrounding water temperature is significantly increased due to the significantly long pulse duration under nanosecond laser irradiation. Since the high peak power is favorable for the formation of defects on the crystal surface, the melting threshold of gold nanorods under femtosecond laser irradiation (about 0.001 J/cm^2) is 99% lower than that under nanosecond laser irradiation (about 0.1 J/cm^2). By comparing the experimental results under femtosecond and nanosecond laser irradiations on gold nanoparticles, the difference in the photothermal conversion characteristics of gold nanoparticles under different pulsed laser irradiations are further analyzed. The results show that when the temperature of the gold nanorods reaches the threshold, the shape of the gold nanorods changes under femtosecond laser irradiation, while the morphology of the gold nanorods changes under nanosecond laser irradiation. The results here have important guiding significance for

the future experiments of high intensity pulsed laser ablation of metal materials.

Key words laser technology; gold nanorods; laser induced optical breakdown; photothermal effect; electron-phonon double temperature model

OCIS codes 140.3380; 160.4236; 170.1610; 170.1870